DOE/ID/12626-4
(DE89017426)
Distribution Category UC-311

DOE/ID/12626--4

DE89 017426

ORDERED CERAMIC MEMBRANES

Annual Progress Report
May 1988 - May 1989

by
Principal Investigators
Marc A. Anderson - Water Chemistry Program
Charles G. Hill, Jr. - Chemical Engineering Department

Staff
Walter A. Zeltner - Postdoctural Associate
Research Specialists
Michal Bursa (Feb. 88 - Present)
Jonathan Patlak (Feb. 89 - Present)
Graduate Research Assistants
Qunyin Xu (Mar. 87 - July 87)
Mary Gieselmann (Mar. 87 - Present)
Reid Peterson (Sep. 88 - Present)

June 1989

Work Performed Under Contract No. DE-AS07-86ID12626

Prepared for
U.S. Department of Energy
Sponsored by the Office of the Assistant Secretary
for Conservation and Renewable Energy
Office of Industrial Programs
Washington, DC

Prepared by
University of Wisconsin - Madison
Madison, Wisconsin 53706

Ordered Ceramic Membranes - Year 3 Progress Report

M.A. Anderson and C.G. Hill

ABSTRACT

As in the first two years of this project, research during the third year covered three major areas: preparation and characterization of supports for the membranes; preparation and characterization of the membranes themselves; and determination of the behavior of systems in which the membranes are attached to supports.

The primary interest in supports was to develop formulations which would provide more reproducible permeabilities (flux of water through the support). Several different clay formulations have been shown to give quite reproducible permeabilities, with the actual permeability varying by nearly an order of magnitude among the different formulations. Supports with smoother surfaces were also fabricated, but rejection studies which compared membranes coated on these supports to membranes coated on rougher supports did not show any significant differences.

Ceramic membranes have been prepared which are composed of three different materials: alumina, titania and silica. Conditions used for synthesizing these membranes have been discussed in the two previous annual reports, but further characterization of these materials as unsupported membranes (membranes which have not been used to coat a support) has been undertaken. A scanning electron

microscopy study of the effect of sintering temperature on the microstructure of unsupported alumina membranes showed that major changes in structure did not occur until sintering temperatures exceeded 1000°C. Such temperatures are associated with a phase transformation to α-alumina. Nitrogen adsorption studies of unsupported silica membranes were used to determine the effects of several preparation parameters on the pore structure of the membranes. The pore structure was relatively unaffected by the solvent used, but higher sintering temperatures gave both smaller pore radii and smaller surface areas. Larger pore radii and smaller surface areas were generally obtained by using either smaller Si/ammonium mole ratios or higher silica solids concentrations in the systems.

The primary focus of titania studies was on synthesizing sols which contained smaller TiO_2 particles. A separate investigation used electrophoretic mobility studies of particles in boehmite sols to determine the effect of phosphate additions on the surface properties of the separate particles. This study showed that additions of up to 10^{-3} M phosphoric acid to these systems had almost no effect on either the surface charges of the particles or the pH of the systems.

Systems in which alumina membranes are coated on clay supports have continued to be characterized by their ability to separate aqueous polyethylene glycol solutions of 1,000 molecular weight. This study is continuing in an attempt to reproduce the high rejections (>90% after 12 coatings of alumina) described in the previous annual report. It was found that the removal rate of the

clay supports from the boehmite sols has a significant effect on the observed rejections. Automating the removal process, which had the effect of slowing the withdrawal rate, led to both higher rejections and a significant increase in reproducibility of results as compared withdrawal by hand. However, rejections in the 80-90% range could be obtained only if the membranes had been previously hydrated by exposure to water under quiescent conditions for several hours or by exposure to a flow of water (dynamic hydration) for about an hour. In a companion study, the effect of gas entrapment within the pore structure was investigated using ultrasound. No effect was observed. Hence we concluded that ceramic membranes require hydration in order to achieve higher rejection levels.

Table of Contents

I. Executive Summary

In this, the third year of this project, we have continued to improve on the performance and reproducibility of our ceramic membrane systems. We have also begun testing these materials using commercially interesting feed stocks. Although we have spent considerable time worrying about reproducing the performance tests of our membranes on 1000 molecular weight polyethylene glycol solutes, this work has uncovered a significant finding for the project with implications for the eventual commercial applications of these membranes. Hydrations turns out to be crucial in these systems; the membranes need to be pre-equilibrated with water if high rejections are to be achieved. The fact that water molecules have been known to form organized structures at the interface of these hydrophilic oxides and the surrounding solution helps us to understand these results. While dynamic equilibration with water may accelerate this process, this equilibration process would be a normal step in a membrane regeneration process.

While we have tried various types of clays and metal oxides in fabricating our supports, we have chosen to use the clay formulation which is described in the report. We have also optimized the coating process in that we now lay down each of the desired 12 layers of the coating material using a carefully controlled rate of withdrawal of 16cm/min. This process yields an alumina membrane which gives maximum rejection of PEG. We have achieved these results without using a "sandwich" layer which would be necessary if a slip-casting method were to be employed.

While we continue to study the highly successful alumina system, we are making progress on titania and silica systems as well. This report contains some new information on both of these systems. The alumina system has not allowed us to obtain a mean pore size below 20 angstroms in radius. By contrast, the titania and silica systems allow us to produce much smaller particles and therefore smaller pores in our ceramic membranes. The formulations needed to produce smaller particles (< 50 Angstroms) in both the silica and titanium systems are under intense investigation and we will not elaborate on these exciting new findings in this report except to conclude that we have been able to produce these extremely small particles by varying the oxide precursors and the process of their hydrolysis.

In future studies, membranes will continue to be tested on whey proteins, beer haze, and other commercially interesting streams. We must find ways of coating small particulate membrane systems onto supports without cracking during calcination. Investigations on whether there are quicker ways of producing supported membranes such that we may avoid some of the time delays necessary in forming multiple coatings and using multiple firings are in progress. We also plan to construct a modular system having a large surface area to volume ratio in cooperation with Oak Ridge National Laboratory. Oak Ridge and the Idaho National Engineering Laboratory are both participating in a cooperative effort to further characterize our membranes in dynamic tests.

II. Supports

A. Fabrication of Clay Supports with Reproducible Characteristics

The problem of fabricating clay supports with reproducible flow characteristics in order to facilitate comparisons of membrane permselectivity characteristics was discussed in the Year 2 Progress Report. This section and the data in Table 1 summarize the results obtained in this study. All clay supports were fabricated by slip casting aqueous suspensions of various clay mixtures into gypsum molds (fabrication of these molds was described in the Year 1 Progress Report). The clay formulations used are all variants of the following basic formula: 4 parts by weight water; 2 parts by weight coarse clay (the type of clay was varied in different formulations); 1 part by weight fine clay (ball clay (OM-4) was used exclusively); sodium carbonate (0.5 to 1% by weight of a 0.5 M solution); sodium silicate (0.3% by weight of a solution of 1 drop of commercial "water glass" in 10 mL of water). Two parts by weight of coarse clay and one part by weight of fine clay give a well packed bulk material. Supports made from clay particles of uniform size do not pack as well and display higher water fluxes.

The clay suspension must hydrolyze for at least two days before casting, and the suspension must be kept in the mold for exactly the same time during each cast (between 1 and 3 minutes). However, sieving the clay mixture to remove very coarse particles

was not found to affect the behavior of the supports. Addition of small quantities of bentonite to the clay mixture (to increase the packing density of particles and the viscosity of the clay suspensions) has not proven beneficial to date. Table 1 summarizes the results obtained for the different types of clay supports which appear to be potentially useful. For these supports the permeability data indicate that 1000 °C is the optimum temperature for firing.

Table 1. Variations in Permeability for Supports Prepared Using Different Clay Formulations.

Sample	Coarse Clay Used	Sieve Mesh	Sample Size	Average Water Flux ($cm^3/cm^2/min$)	Standard Dev. Water Flux
1	AP Green	230	7	0.071	0.004
2	AP Green (*)	230	4	0.057	0.004
3	AP Green	170	7	0.067	0.004
4	Hawthorne Bond	230	4	0.044	0.007
5	Yellow Banks (*)	325	6	0.169	0.020

(*) Approximately 3% by weight of bentonite was also employed in this formulation.

Supports used for other studies in this project have been prepared using sieved AP Green clay. However, it is desirable for the support to have as low a resistance to flow as possible. Therefore, we plan to perform a rejection study to compare coated AP Green supports with coated Yellow Banks supports to determine

if the membrane cast on the Yellow Banks supports have superior permselectivity characteristics.

B. Preparation of Supports with Smoother Outer Surfaces

The clay supports used in this project are fabricated in the same shape as test-tubes. The supports are coated with sol by dipping the support into the sol. Since the supports are coated on their outer surface, it is possible that the roughness of this outer surface influences the water permeability of the composite material and the concomitant rejection characteristics associated therewith.

Scanning electron microscope (SEM) pictures of the outer surface of uncoated supports show that the surfaces are rough on a scale of microns. Several attempts have been made to prepare supports with smoother outer surfaces.

1. Three supports included in Sample 3 mentioned above were hand polished and coated with 5 layers of alumina. However, the water permeabilities of these hand polished supports were indistinguishable from those of similar membranes supported on non-polished supports fabricated in the same batch. No further characterization tests were performed on these supports.

2. A clay suspension was ball-milled for 24 hr. Supports were then prepared from this suspension by slip casting. SEM pictures of the outer surfaces of these supports appeared virtually identical to the SEM pictures mentioned above. Hence, no further

characterization tests were performed.

3. A clay suspension was thinned with water, and a dry unfired (green body) support was quickly dipped into the diluted suspension. SEM pictures indicated that an extremely thin layer of clay was deposited on the outer surface of the support, clearly producing a smoother surface. However, supports containing this extra layer of clay (sandwich layer) must still be further characterized.

The idea of using a thin sandwich layer as a transition between a support surface with large pore sizes and a membrane with very fine pores is quite common in the field of ceramic membranes. We have been able, possibly fortuitously, to prepare supported alumina membranes with very good rejections without having to resort to this extra fabrication step. Consequently, studies of the effects of a clay sandwich layer are not currently a high priority for us in our work with alumina membranes. In fact, the preparation of clay supports as described above may provide a type of sandwich layer without the need for an extra fabrication step. When the clay suspension is poured into the mold, the resulting arrangement of particles is determined by both gravity and capillary forces. Capillary forces are more important, and more of the fine material is deposited on the outside of the supports than on the inside leading to the natural formation of a sandwich layer.

III. Unsupported Membranes

A. Alumina

1. Effect of Sintering Temperature on the Microstructure of Unsupported Alumina Membranes

Ten boehmite xerogels were prepared from a standard sol: $[Al]_T$ = 0.5 M, HNO_3/Al_T = 0.07 mole ratio, and pH_{final} = 3.9. Nine of the gels were fired to different temperatures between 425 and 1600°C (See Fig. 1).

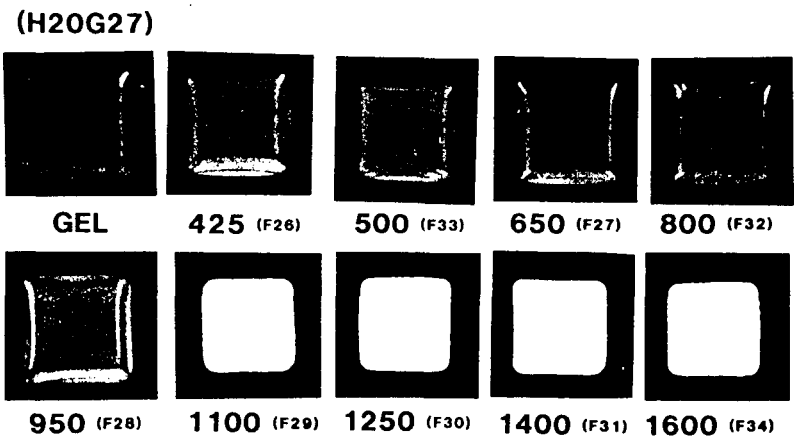

Fig. 1. Effect of sintering temperature on the general appearance of unsupported boehmite gels and alumina membranes.

A phase transformation between boehmite and γ-alumina occurs around 500°C. Transition alumina phases persist up to 1100-1200°C, where a major atomic rearrangement leading to α-alumina occurs. This last change is accompanied by significant grain growth. As a result of these changes, the samples shrink and gradually change in appearance from clear to translucent to opaque white.

Results of N_2 sorption measurements are given in Fig. 2, which shows the effect of sintering temperature on the surface area and pore structure of these samples.

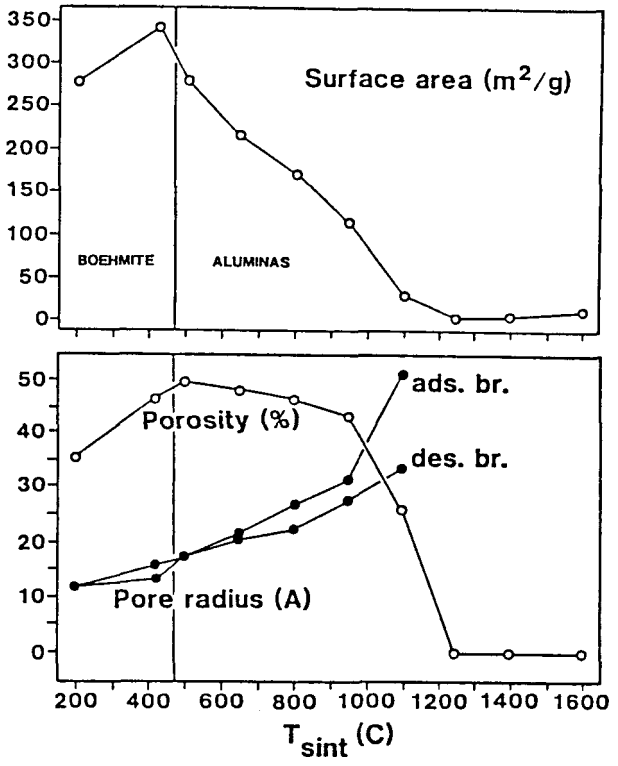

Fig. 2 Effect of Sintering on Surface Area and Pore Size of Boehmite Gels and Alumina Membranes. The data for temperatures greater than 1100 °C are misleading - see text.)

In general the surface area decreases with increasing sintering temperature. Between 425 and 950°C the porosity remains fairly constant (43-49%), but it falls to 0% at 1250°C and higher. Although this loss of porosity might be due to pore closure, this idea is contradicted by the fact that the radius of the pores actually grows with increasing sintering temperature. SEM pictures of these samples show that, at sintering temperatures $\leq$1100°C, the

microstructure of the membranes is composed of small spherical aggregates (Fig. 3). At sintering temperatures above 1100°C, significant grain growth occurs with a concomitant increase in pore size (Fig. 4). Since significant amounts of capillary condensation cannot occur in such large pores, the N_2 sorption measurements indicate that no pores are present, thus erroneously leading one to believe that the samples are non-porous.

Fig. 3. SEM of fracture edge of Al_2O_3 membrane sintered at 500 °C. This microstructure is typical of sintering temperatures below 1100 °C. (Size bar = 1 μm)

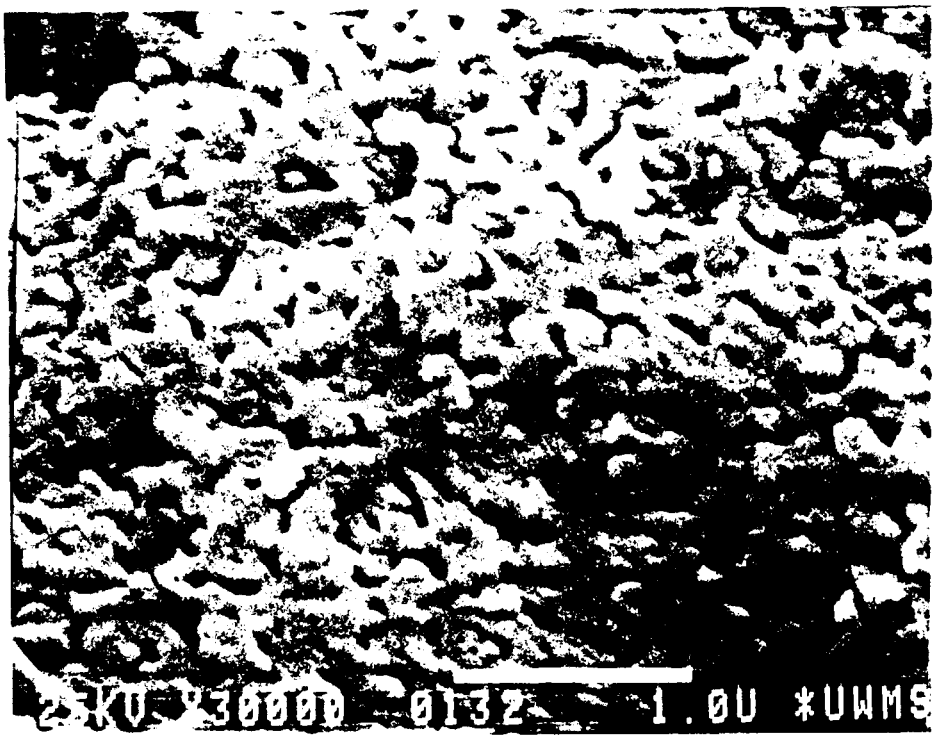

Fig. 4. SEM of fracture edge of Al_2O_3 membrane sintered at 1250°c. (Size bar = 1 μm)

2. Effect of Solids Concentration in the Sol on the Properties of the Resulting Membrane

In silica sols prepared by the Stöber process, an increase in both particle and pore size is known to result from an increase in solids concentration in the sol. Consequently, an experiment was performed to see if the same phenomena occur in the boehmite/alumina system. Four sols with different solids concentrations were prepared while holding the HNO_3/Al_T mole ratio constant at 0.07 (see Table II). The sols were then either concentrated or diluted to solids concentrations of 2.2 wt%. Aliquots of these sols were gelled in the usual manner and the resultant membranes were fired to 500°C. The results of the N_2

sorption measurements on these samples are indicated in Table II. As can be seen, there is no obvious effect of the solids concentration in the precursor sol on either the surface area or pore radius of γ-alumina membranes.

Table II. Effects of Solids Concentration in the Precursor Sol on the Pore Structure of Unsupported Membranes of γ-Alumina.

Sample	Solids Content of original sol (wt%)	Properties of Membrane Fired at 500°C Porosity (%)	Surface area m^2/gm	Pore radius (Å)
A	0.55	51.0	303	17.5
B	1.1	47.8	285	17.8
C	2.2	49.7	306	16.8
D	4.4	51.7	312	17.5

B. Silica

For characterization of the pore structure of unsupported silica membranes, the adsorption branch of the BET isotherm proved to be too broad to provide an acceptable indication of the true pore size and distribution. Therefore, the mean pore radius is reported determined from the desorption branch of the isotherm was used exclusively as a measure of this parameter in our work with silica membranes.

1. Preparation

Ethanolic suspensions of silica particles were obtained by the hydrolysis of tetraethyl orthosilicate (TEOS) in ammonium hydroxide (NH_4OH). All unsupported silica membranes were prepared by slow evaporation at room temperature. Four major parameters were examined to determine their effects on particle and membrane properties. They are as follows:

A. Type of gelling solvent - EtOH vs. H_2O vs. sonicated H_2O;

B. Silica/ammonia mole ratio - TEOS/NH_4OH during hydrolysis;

C. Solids concentration - % (wt/vol) SiO_2 in solution;

D. Sintering temperatures - 200-1000 °C

2. Solvent Effects

The general appearance of the sols did not differ appreciably from ethanol, regardless of whether water or sonicated water was used as the gelling medium (see Year 2 Progress Report). The data obtained from nitrogen sorption determinations support the conclusion that type of solvent employed had little effect on either the porosity or the pore size distribution. Table III reflects the resulting similarities.

3. Silica/ammonium mole ratio:

The TEOS/NH_4OH mole ratio was decreased by increasing the concentration of NH_4OH while the solids concentration remained stable at ≈ 2% (wt/vol). This change produced progressively cloudier sols and xerogels. Table III and Figure 5 show pore size

to be inversely related to the silica/ammonia mole ratio. The data plotted in Figure 5 indicate that mean pore radius increased as the Si/NH_3 mole ratio decreased, irrespective of the type of solvent employed. In Table III, the data for sample #4 was questioned since it did not fit the sequence of results, but replicate sample, #27, did follow the general pattern described above.

Table III: Effects of Gelling Solvent and Silica/Ammonia Mole Ratio on the Pore Structure of Silica Membranes

#	Label	Si/NH_3 mole ratio	Solids (%,wt/vol)	Surface Area (m^2/gM)	Pores (%)	Radius (Å)
1.	HS 5G30E	1.51	1.96	758	68.3	31
2.	HS 6G30E	1.01	1.95	557	67.3	48
3.	HS 7G30E	0.76	1.93	379	61.5	68
4.	HS 8G30E	0.61	1.92	305	62.0	114
27.	HS 8BE	0.61	1.92	231	44.6	57
24.	HS 9G30E	0.50	1.91	231	51.6	88
25.	HS10G30E	0.43	1.89	188	46.9	89
26.	HS11G30E	0.38	1.88	62	40.5	90
5.	HS 5G30W	1.51	1.96	528	67.4	35
6.	HS 6G30W	1.01	1.95	440	66.9	51
7.	HS 7G30W	0.76	1.93	313	57.3	81
8.	HS 8G30W	0.61	1.92	271	56.7	93
9.	HS 9G30W	0.50	1.91	257	50.6	90
10.	HS10G30W	0.43	1.89	247	48.2	94
11.	HS11G30W	0.38	1.88	220	44.4	95
12.	HS5G30S	1.51	1.96	577	67.1	33
13.	HS6G30S	1.01	1.95	438	68.1	50
14.	HS7G30S	0.76	1.93	269	59.3	75
15.	HS8G30S	0.61	1.92	266	53.7	94
16.	HS9G30S	0.50	1.91	128	34.5	94
17.	HS10G30S	0.43	1.89	246	48.6	100
18.	HS11G30S	0.38	1.88	229	46.0	100

[+] **E** = Ethanol, **W** = Water, **S** = Sonicated Water

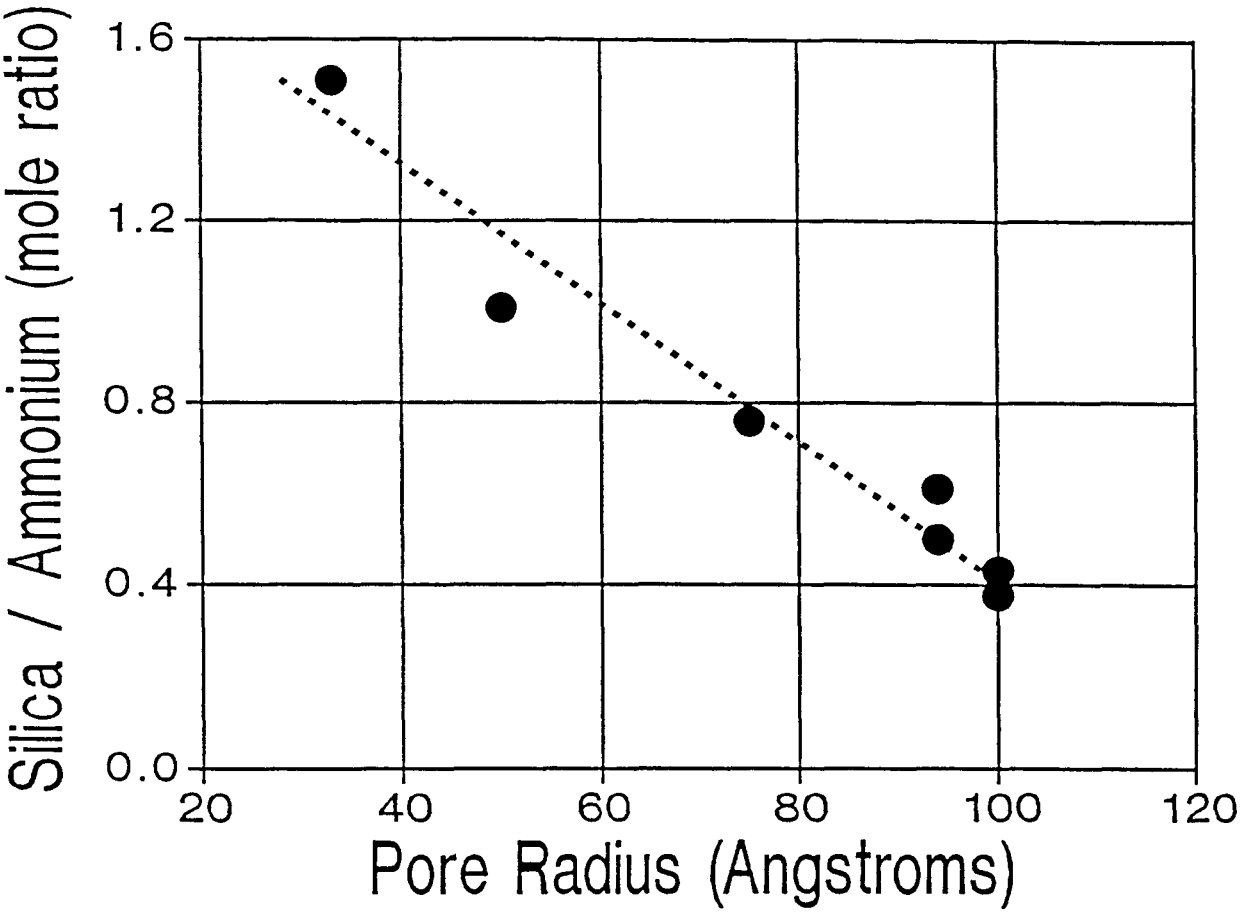

Fig. 5. Effect of Silica/Ammonium Molar Ratio on Pore Size

4. Solids concentration

The percentage of silica was increased while the Si/NH_3 mole ratio was kept constant at 1.21. Again, the visible effect was seen in the formation of progressively cloudier sols and xerogels. Inspection of data in Table IV and Figure 6 reveals that the pore size was linearly related to the solids concentration. The mean

pore radius increased as the solids concentration increased. Since our objective was to create membranes with small pore sizes, the following experiments were conducted.

1. Sols #31 and #28 were concentrated (by factors of 3.33 and 7, respectively) via rotary evaporation prior to membrane formation. Later, these sols were resuspended by diluting them to their original volume with ethanol and sonicated to simulate their original solids concentration. Table IV shows that the diluted sols formed membranes, #40 and #39, that have mean pore sizes very similar to those of their more concentrated counterparts.

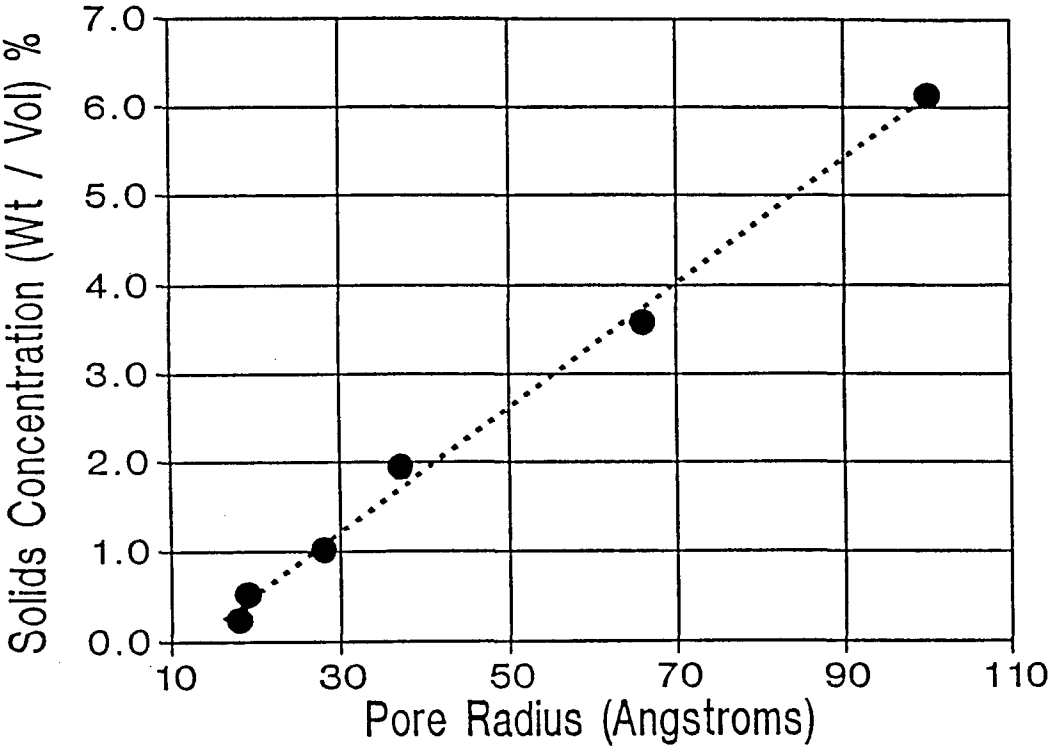

Fig. 6. Effect of Solids Concentration on Pore Radius

2. We next reproduced sols #31 and #28. This time however, we then concentrated these sols by a factor of two giving us sols labeled #38 and #37. They yielded membranes that had significantly smaller mean pore radius than had been produced up to this point.

Scanning electron microscopy was employed to distinguish structure and to estimate particle size ranges. The data in Table V show that as the solids concentrations is increased from 0.52% in sample #19 to 6.14% in sample #23, the mean radius of the particles increases from ≈40 nm in #19 to ≈200 nm in #23. When sample #31 was prepared, we were able to confirm our hypothesis that more dilute sols give membranes composed of smaller particles.

5. Sintering temperature

Four identical samples were fired at four different temperatures. Table VI and Figure 7 demonstrate that the pore radii enlarge from 42Å to 58Å when a firing temperature of 400 °C is employed. When the samples are fired at 1000°c, however, the mean pore radius decreased considerably to 29Å. This decrease was accompanied by a loss of more than half the porosity of the sample.

Table IV: Effects of Solids Concentration on Specific Surface Area, Porosity and Mean Pore Size

#	Label	[Solids]$^{\alpha}$ (original)	[Solids]$^{\beta}$ (gelling)	Surf. Area m^2/g	Porosity (%)	Pore Radius (Å)
31.	HS22BE	0.25	1.67	739	57.5	18
28.	HS16BE	0.52	1.74	675	66.2	28
29.	HS18BE	1.95	-	541	66.8	42
30.	HS20BE	6.24	-	227	35.9	10
38.	HS22CE	0.24	0.48	775	57.2	11
37.	HS16CE	0.52	1.05	710	59.6	18
40.	HS22BE	1.67	0.24	707	62.4	19
39.	HS16BE	1.74	0.52	647	66.9	34

$^{\alpha}$ [Solids] = % (w/v) SiO_2 in suspension as originally prepared.

$^{\beta}$ [Solids] = % (w/v) SiO_2 in suspension at the start of gelation.
(- means unchanged)

Sample number	Unsupported Membrane Preparation
31.	concentrated to 1/3 original sol volume
28.	concentrated to 1/7 original sol volume
38. & 37.	concentrated to 1/2 original sol volume
40.	diluted with EtOH by factor 3.33 to simulate original sol 31
39.	diluted with EtOH by factor 7.00 to simulate original sol 28

Table V: Effects of Solids Concentration on Particle Size, Specific Surface Area, and Mean Pore Size

#	Label	[Solids] (%,wt/vol)	Particle Range(nm)	Surf. Area (m^2/g)	Pores (%)	Radius (Å)
31.	HS22BE	0.24	<30 - 50	739	57.5	18
19.	HS16G34W	0.52	35 - 70	681	63.5	19
20.	HS17G34W	1.02	50 - 85	1296	78.1	28
21.	HS18G34W	1.95	35 - 85	483	64.8	37
22.	HS19G34W	3.58	100 - 135	257	53.8	66
23.	HS20G34W	6.14	135 - 200	208	45.8	100

Particle size range estimated from Scanning Electron Micrographs

Table VI: Effects of Sintering Temperature on Specific Surface Area, Porosity, and Mean Pore Radius

Sample	Label	Sint.Temp. (°c)	Surf. Area (m^2/g)	Poros. (%)	Radius (Å)
29.	HS18BE	(200)	541	66.8	42
32.	HS18BE.400	400	664	69.7	58
33.	HS18BE.600	600	476	66.8	54
34.	HS18BE.800	800	310	62.6	52
35.	HS18BE1000	1000	82	28.9	29

Sample 29 was not fired but was evacuated @ 200°C during the BET study.

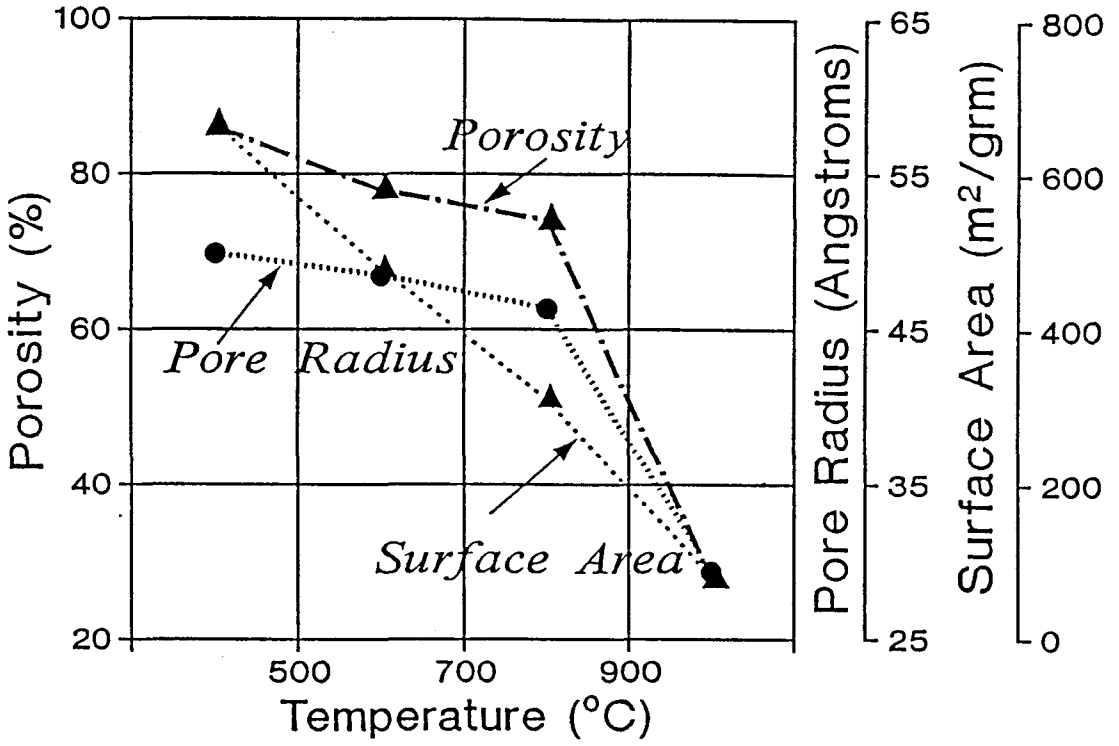

Fig 7. Temperature Effects on Porosity, Radius and Specific Surface Area

C. Titania

Particulate TiO_2 membranes were prepared by the sol-gel technique, starting with titanium tetraisopropoxide. The procedure (see Year 2 Annual Report) includes: (1) preparation of suspendable TiO_2 precipitates by hydrolysis of $Ti(i\text{-}C_3H_7O)_4$ in aqueous medium; (2) preparation of a stable colloidal suspension through peptization of the precipitates with HNO_3; (3) gel formation through evaporation of water; (4) drying of the hydrogel to a crack-free xerogel under constant relative humidity at room temperature; (5) production of unsupported TiO_2 membranes by firing xerogels at 250°C to 500°C. Chemically pure grade materials were used as received without further purification. Average particle sizes in various sols were measured by quasi-elastic light scattering (QELS). The data were chosen as the averages of the results of several measurements taken at angles from 150° to 30°. The primary particle sizes in TiO_2 sols were determined from TEM images of the corresponding gels. Pore size distributions in membranes were measured by N_2 adsorption, assuming that pores are cylindrical in shape.

1. Hydrolysis and Peptization

The preparation of TiO_2 lyophobic sols was conducted in two stages: 1) hydrolyzing titanium tetraisopropoxide in an aqueous system; and 2) peptizing the resulting TiO_2 precipitates with appropriate amounts of HNO_3. Final particle sizes and

polydispersities are determined by processing conditions in both stages. Two main experimental variables, pH and temperature, affect the nature of the precipitates produced during the hydrolysis stage. Table VII indicates that hydrolysis in acidic solution (pH 1.12 at 25 °C) produces smaller particles in the peptized sol. A reduced primary particle size or a loose agglomerate structure which would break into smaller particles would both result in small particles in the final sol. Therefore, both the amount of acid utilized to catalyze the reaction and the reaction temperature play important roles in this process. These effects are manifested from hydrolysis and condensation of initial reactants, through nucleation and particle growth, to agglomeration and precipitation.

TABLE VII. Preparation Conditions and Characterization of TiO_2 Colloidal Sols

*Sample	Hydrol. Condt.		Peptizing Conditions			**Part.Size Diameter (by QELS)	Final pH in Sols (Measured)
	pH	Temp.	pH	Temp.	Time		
A	6-7	25±2°C	0.99	85±2°C	10 hrs	20±1 nm	1.14
B	1.12	25±2°C	1.12	25±2°C	66 hrs	16±1 nm	1.49
C	6-7	65±2°C	0.99	85±2°C	10 hrs	123±4 nm	1.16

*All samples have a particle concentration of 22.2g TiO_2 / l .
**All samples were sonicated before particle size measurements.

Peptization can also affect the nature of the particles in the final sols. Peptization is a common method for preparing stable colloidal suspensions from bulk matter. This procedure involves three possible processes which can occur simultaneously: 1) disintegration of agglomerates into particles of colloidal dimensions as a result of thermal or mechanical phenomena; 2) charging of particles by proton adsorption which, in turn, stabilizes the suspension through electrostatic repulsion effects; 3) reaggregation of particles caused by collisions to give larger, but more weakly bound, aggregates whose sizes remain in the colloidal range. The overall process of peptization is complex and the average particle size of the end product will depend on the relative rates of the disintegrations and aggregation processes. In peptization, a number of factors must be considered: 1) pH of the solution - this factor determines the surface potential of the particles; 2) ionic strength - this variable controls the thickness of the double layer surrounding the particles; 3) particle concentration - the greater the density of particles the higher the probability of collision; 4) temperature - this variable not only provides the energy for breaking apart precipitates but also for reaggregating the resultant particles. Figure 8 indicates how the average particle sizes, measured by quasi-elastic light scattering, varies with the concentration of the peptizing acid (expressed by the mole ratio of acid to titanium) for three sol concentrations.

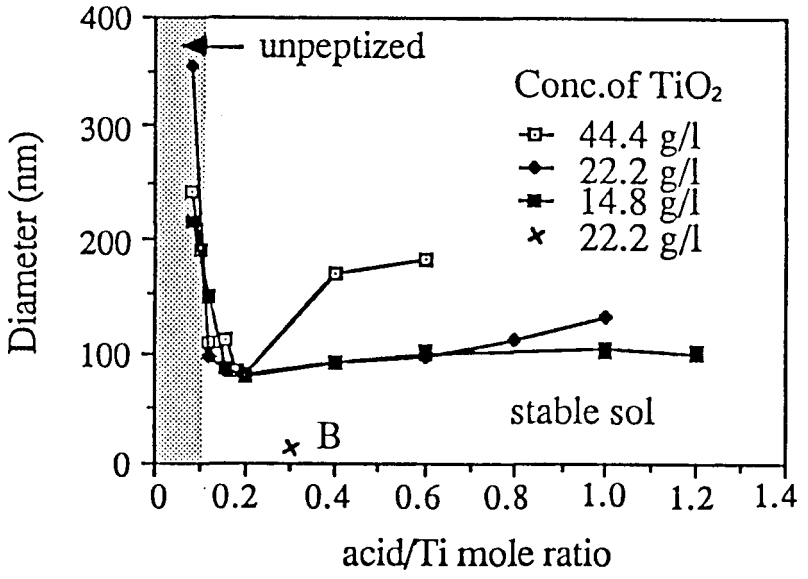

Fig 8. Average Particle size in various sols. Three curves have the same hydrolyzing conditions as sample A in Table VII. Point B has the same hydrolyzing conditions as sample B. All samples were peptized at 85°C.

All three curves drop off rapidly with initially increasing H+/Ti mole ratio, then pass through almost the same minimum point (where H+/Ti=0.2, diameter= 80 nm), and finally increase with increasing acid concentration. This final increase of aggregate size is caused by the increase in the overall ionic strength of the solution in the region of higher acid concentration. Point B in Fig. 8 corresponds to the average particle size in the sol which was peptized at 25°C for 66 hours. While higher temperatures promote formation of larger aggregates, these aggregates can be easily disintegrated by sonication, reducing the net aggregate size to 19-20 nm.

2. Gelation

The sol to gel transformation takes place during evaporation of water from the sol. However, evaporation does not always produce gels, as precipitates which yield powders upon drying are obtained in many cases. Although both gels and precipitates are products of destabilization of a sol, a gel is defined as a semi-solid system with a continuous particle network throughout the whole dispersion medium. Failure to produce such a network during aggregation will lead to precipitation. In order to obtain a gel, the effects of pH and ionic strength during volume reduction must be to stabilize the particles until the volume reaches a point where the interactions of the electric fields around the particles are so strong that the particles are prevented from moving together to coagulate.

Gelation experiments were conducted using sols A,B and C described in Table VII. Samples A and C form complete gels upon evaporation of water, while Sample B yields part gel and part powder. However, if Sample B is dialyzed to pH 2.9, it will gel completely. This result seems to indicate that smaller particles tend to gel under more moderate conditions (i.e., lower ionic strengths). Particle packing geometry during gelation is another factor which could influence the final membrane pore structure. In conventional colloidal sols made by the sol-gel method, particles can exist as monodisperse primary particles, as small aggregates composed of two or three primary particles, or as large aggregates in which more than four primary particles combine together, thereby forming primary pores between them. Figure 9

illustrates three possible gel structures derived from sols containing different degrees of aggregation.

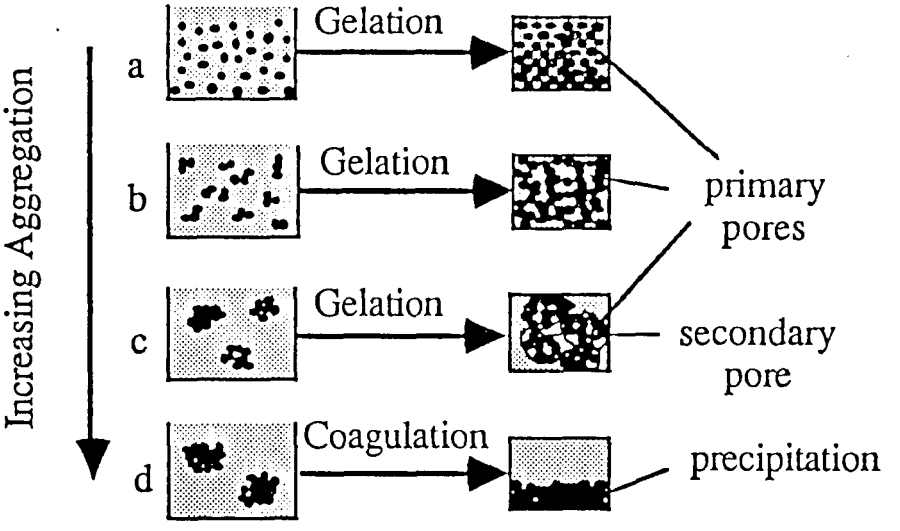

Fig 9. Increasing degrees of aggregation in the sols from (a) to (d) leads to three types of gels and precipitation.

Uniform primary particles tend to pack densely to produce micro-sized primary pores between the particles (Fig. 9a). Small aggregates are likely to gel with looser packing geometry, producing large sized primary pores (Fig. 9b). Large aggregates are packed most loosely, forming macro-sized secondary pores or open channels between aggregates, with the meso-sized primary pores remaining inside these aggregates (Fig. 9c). All of the TiO_2 sols derived from peptization at 85°C contain large aggregates. Their packing geometries fall into category (c). However, the sonicated sols may have type (b) structures since they contain small

aggregates. None of the sols obtained so far contain monodisperse primary particles.

3. Pore Structures of Membranes

Do sol chemistry and gel structure determine the mean pore size of the ultimate membranes? Table VIII shows the results of N_2 adsorption various measurements for membranes. Samples A,B and C were prepared from sols A,B and C described in Table VII. Sample A-1 was derived from a non-sonicated portion of sol A. Comparison of the data for samples A, B and C indicates that the mean pore sizes increase with both increasing primary particle sizes and aggregate sizes. The results obtained for samples A and A-1 are somewhat unexpected. These sols contain the same size primary particles but different size aggregates. They should lead to different packing structures in their hydrogels. However, after drying and firing under identical conditions, they lead to the same mean pore size in the final membranes. This result indicates that during drying, particles tend to pack more densely rather than maintain the packing geometry of the wet gel. This collapse of the hydrogel structure is probably caused by the formation of gas-solid interfaces (which are characterized by a larger surface tensions than are water-solid interfaces) by elimination of water during drying. The decrease in free energy resulting from a reduction in interfacial area causes shrinkage of the gel as the particles rearrange to give a configuration with minimal free energy. Therefore, the primary particle size, rather than the aggregate

size, may be the key factor in determining the mean pore sizes of the final membranes.

TABLE VIII. Relationship Between Particle Sizes in Sols and the Mean Pore Size in Membranes.

Sample	Primary Size in Diam. (by TEM)	Aggreg. Size in Diam. (by QELS)	Mean Pore Size* in Diam. (by BET)
A-1**	7±2 nm	85±3 nm	2.4±0.2 nm
A	7±2 nm	20±1 nm	2.4±0.2 nm
B	3±1 nm	16±1 nm	1.8±0.2 nm
C		123±4 nm	3.0±0.3 nm

* All gels were fired at 250°C for 0.5 hrs before BET measurements.
** A-1 has a same chemical composition and preparative conditions as sample A except sonication before gelation.

IV. SUPPORTED MEMBRANES

A. Slip-Casting an Alumina Membrane.

To date, the alumina membranes have been applied by a procedure which involves dipping a water-soaked clay support into a 3 wt% boehmite sol. To see if a membrane could be slip-cast, a dry support which had received a thin clay "sandwich" layer (see Section IIB.) was dipped into a 6 wt% boehmite sol for 30 secs. The tube was then fired and examined by SEM. Fig. 10 indicates that a membrane was definitely formed and that it was 5-10 μm in thickness. Mosaic cracking occurred in the membrane (See Fig. 12).

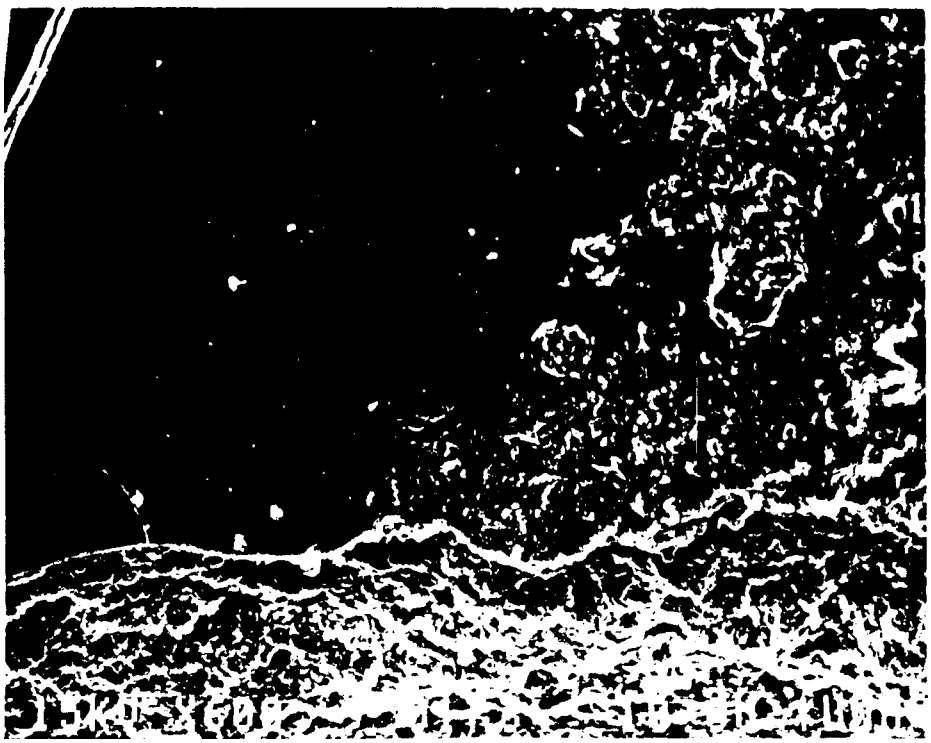

Fig. 10 SEM of top surface of clay support at the interface between the uncoated support (top of image) and slurry coating (bottom of image). (Size bar = 10 microns)

This cracking could be explained either by the formation of too thick a membrane when it was cast in a single step or by a situation in which the membrane gelled and dried too quickly. A comparison of dipped membranes and those formed by slip-casting as a function of time and sol concentration is presently under way.

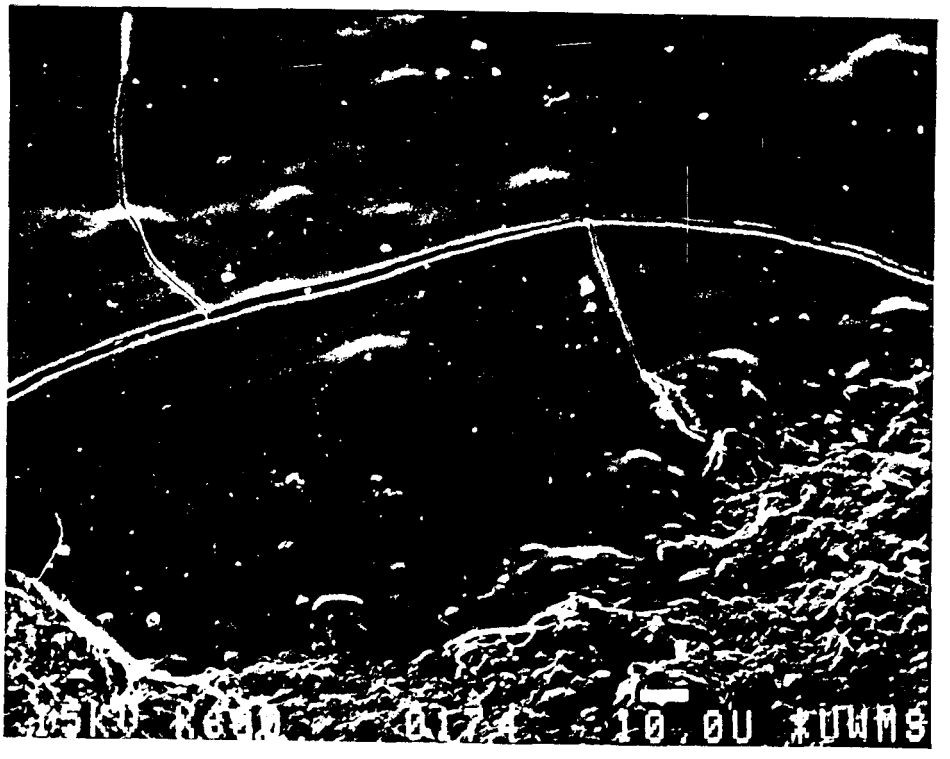

Fig. 11 SEM of the top surface (taken at a slight angle off perpendicular) of the interface between an alumina membrane and a slurry-coated clay support. (Size bar = 10 microns)

B. Effects of Phosphate Treatment on Alumina Sols.

These sols were characterized by their pH, the mobility of the alumina particles and the permselective properties of the resulting membranes. Tables IX-XII illustrate how these characteristics change with time. All supports were coated by dipping them 5 times into the sols. After dipping the coated supports were allowed to air dry. These coated supports were then fired at 500°C. This sequence of coating, drying and firing was then repeated. All supports were hand withdrawn from the sols. Permeabilities are measured in $cm^3/cm^2/min$ and mobilities in 10^{-8} $m^2/V\text{-}sec$, while water permeability refers to measured the flux of water through the given support before it is coated.

The alumina sols containing phosphate seem to be stable over time, as the particle mobility and pH do not change significantly even after several months. In several experiments, supports were coated with sols aged for 8 days, 3 weeks, 1 month, and 3 months. The membranes formed from these sols were then tested for the rejection of polyethylene glycol (PEG). The rejection was better for membranes derived from sols aged for one month and three months. Supports coated with a one month old sol containing 10^{-5} M phosphate gave relatively good rejections (Ca 50%) which increased when these supported membranes had been previously hydrated. The mobility did not change appreciably over the course of these experiments and therefore was not measured in every case.

Three important issues affect the results of these studies: these supported membranes were not hydrated, they were hand dipped, and it is clear that the amounts of phosphate added were not large enough to significantly affect the boehmite particles. This study will be repeated using larger phosphate loadings to produce a noticeable change in the aggregation state of the system.

Table IX. Effect of Phosphate on Electrophoretic Mobility Values and Rejection Characteristics of Membranes Prepared from Boehmite Sols Aged for 8 Days.

Support	Phosphate	Mobility	pH	Water Perm	PEG Perm	R%
D16	10^{-5} M	4.12	4.1	0.114	0.046	32
B16	$2x10^{-5}$ M	4.11	4.2	0.116	0.040	13
A15	10^{-4} M	3.82	4.1	0.118	0.033	17
F15	10^{-3} M	3.96	4.1	0.119	0.053	7

Table X. Effect of Phosphate on Rejection Characteristics of Membranes Prepared from Boehmite Sols Aged for 3 Weeks.

Support	Phosphate	Water Perm	PEG Perm	Rej(%)
F11	0.5 10^{-5} M	0.054	0.021	14
B11	0.5 10^{-5} M	0.051	0.025	12
A14	2 10^{-5} M	0.048	0.024	22
C14	10^{-4} M	0.053	0.021	34
A13	10^{-4} M	0.063	0.029	31
B13	10^{-3} M	0.081	0.031	35

Table XI. Effect of Phosphate on Electrophoretic Mobility Values and Rejection Characteristics of Membranes Prepared from Boehmite Sols Aged for 1 Month.

Support	Phosphate	Mobility	pH	Water Perm	PEG Perm	R%
C21	10^{-5} M	4.07	4.1	0.048	0.021	47
D21	10^{-5} M	4.07	4.1	0.043	0.020	48
E21	10^{-5} M	4.07	4.1	0.047	0.015	41
C20	$2x10^{-5}$ M	4.07	4.2	0.115	0.024	52
C19	10^{-4} M	4.22	-	0.173	0.070	14
E19	10^{-4} M	4.22	-	-	-	18
A20	10^{-3} M	3.93	4.1	0.051	0.01	59

Table XII. Effects of Phosphate on PEG Rejection for Alumina Membranes Prepared from Boehmite Sols Aged 3 Months

Support	Phosphate	Water Perm	PEG Perm	Rejection (%)
A 21	$0.5\ 10^{-5}$	0.055	0.029	28
B 21	$0.5\ 10^{-5}$	0.066	0.026	32
G 21	$2\ 10^{-5}$	0.056	0.016	50
F 21	$2\ 10^{-5}$	0.047	0.026	32
A 23	10^{-4}	0.048	0.023	50
C 23	10^{-4}	0.062	0.024	47
G 23	10^{-3}	0.074	0.024	44

C. Alternative Methods of Coating and Firing

In order to test coating and firing procedures we prepared six supports from the same batch of clay and divided them into two groups. The supports had similar permeabilities with respect to the transport of water before an alumina (10^{-5} M phosphate) membrane was placed on the support. The supports from one group were dried before dipping, received five coatings, and then fired. The supports from the second group were dipped wet and fired after every dip for a total of five coatings. The flow rates for all of these supports were similar. This result indicates that there is no practical difference for these two methods of coating.

D. Importance of Mechanized Coating Procedures

We compared properties of membranes produced from supports which were coated by hand dipping with those of membranes in which the supports were coated using a mechanized withdrawal system. In the hand dipping procedure, the supports were coated simply by dipping the supports into the sol, keeping them there for approximately 20 seconds and then withdrawing them. (Note that the withdrawal rate is somewhat arbitrary in this procedure.) In the mechanized procedure a special instrument was developed to withdraw the supports from the sols at fixed rates of removal. This removal rate could be varied. Table XIII illustrates the importance of this

variable. We have now fixed the removal velocity at 16.7 cm/min.

We have found that there are no further improvements in membrane rejection characteristics after 12 coatings (3 cycles at 4 dippings/cycle and firing between cycles). What we do not know for sure is if one can lay down 12 coatings and fire only once and produce the same effect? We also do not know if systems prepared by placing more concentrated sols on the supports with only one or two coatings can be equally effective?

Table XIII. Effect of Velocities on the PEG Rejection Using an Alumina Membrane Coating Process

Support	Water perm.	PEG perm.	Velocity (cm/min)	Rejection%
H 23	0.061	0.023	7.9	50.6
F 23	0.058	0.022	16.7	57.5
D 23	0.056	0.017	34.1	58.9
E 23	0.057	0.021	manual	34.7

Permeability units - $cc/cm^2/min$ at 25 °C Firing Cycle - 4 coating layers followed by firing, 4 more layers followed by another firing and finally 4 more coating layers followed by a final firing.

E. The Effect of Hydration On Rejection

Ceramic membranes comprised of oxides are in many cases hydrophilic systems and require time to hydrate. When trying to reproduce some of our earlier results on the rejection of PEG, we noticed a much poorer rejection rate (approximately 50% as compared to the nearly 100% earlier achieved for the same membrane systems).

After several months of trying to understand this discrepancy, we finally noticed that the rejections could be significantly enhanced by simply wetting the membranes a week before their use. In hindsight, when we recalled that some of our FTIR work indicated that alumina and titania particles structure water near their surfaces, these results are not surprising. These results mean that ceramic membranes composed of oxides will require a hydration period before being brought onstream in commercial applications.

Results of these hydration studies are given in Tables XIV and XV. The best rejections (80-90%) were obtained with supports which had immersed for 15 days before use. We found that we could reproduce the poor results obtained with dry systems by simply firing the hydrated supported membranes at 500 °C for an hour and then running the rejection study without again allowing them time to undergo hydration. If these same membranes were fired and then equilibrated with water for 15 days it was possible to restore their performance to the higher level. This result means that the membranes can be successfully regenerated but they must be reequilibrated with water after the regeneration process. It should be noted that the 15 day period was arbitrary, and this most likely could be shortened considerably.

Table XIV. Effect of Membrane Hydration on PEG Rejection

Support	cycles	Water Perm	PEG Perm	Rej (%)		PEG Perm	Rej%
HA27	5	0.094	0.025	62	RH	0.008	--
A29	5	0.141	0.030	49	RH	0.009	88
C29	5	0.149	0.029	56	RH	0.010	80
E29	5	0.129	0.025	57	RH	0.011	90
F28	4	0.132	0.024	65	RH	0.010	84
D28	4	0.140	0.027	56	RH	0.009	88
E28	4	0.128	0.023	50	RH	-----	78

Perm. units - $cc/cm^2/min$
R = Regeneration - ramp up and down 1.7°C/min, to 350 °C, dwell time of 0.5 hours, ramp down at same rate to 85°C.
H= hydration - 15 days in deionized water.
Firing cycle represents 4 coating layers and one firing
Velocity of withdrawal - 16.7 cm/min

Table XV. Effect of Membrane Hydration and De-hydration on PEG Rejection

Support	Firing cycles	Water Perm	PEG Perm	Rej (%)	R H	PEG Perm	Rej (%)	R	PEG Perm	Rej (%)
H 27	5	0.094	0.025	62	R H	0.008	92	R	0.009	65
D 28	4	0.140	0.027	56	R H	0.009	88	R	0.012	66
F 28	4	0.132	0.024	65	R H	0.010	84	R	0.013	61
E 28	4	0.128	0.023	50	R H	-----	78	R	0.010	61
E 29	5	0.129	0.025	57	R H	0.011	90	R	0.010	63

R- Regeneration Rate same as in Table XIV.
H-Hydration - 15 days in the deionized water
Firing cycle - 4 coating layers and one firing
Velocity of withdrawal - 16.7 cm/min
Sol-HA27

With continued operation we find as in our last study that permeate rejection drops from approximately 90% to less than 70% after three hours of equilibration. In this study we used a different test solution (1000 MW PEG) than that previously (8000 MW PEG). Dynamic hydration tends to lower the time frame required for hydration which would shorten the total regeneration procedure. Hydration took place in deionized water.The loss of the supported membrane at this pH after 10 weeks is extremely low as was discussed in our last project report. (For an alumina membrane at a pH close to the pH of deionized water we obtain the same pH for both the feed and permeate.)

V. LARGE SCALE PERMEATION TESTING

Progress has been made in two areas. First, longer tubes have been tested in an effort to begin scale up of the system. These clay tubes are made in the same fashion as discussed in section IIA but were longer, varying in length from 16.8 to 19.8 cm. Tests on the tubes have been successful as water permeabilities of coated tubes appear to be the same as those of the smaller tubes. However, selectivity has only been measured for high molecular weight molecules.

One of the large molecules tested was Bovine Serum Albumin. Using an alumina membrane coated on the long clay supports, we achieved rejections from 98.3% to 98.7%. Concentrations of Bovine Serum Albumin in the feed and permeate were measured using total

organic carbon analysis. However, there was enough background carbon in the samples to suggest errors of 1 to 3%, thus, one could assume essentially 100% rejection.

The other large molecule tested was cheese whey protein from cottage cheese whey. Kjeldahl analysis indicated only 75% rejection. However, this was the initial test and it was obvious that there was an error in the analysis. More likely, the rejection was closer to 100%, for when the protein was precipitated out of the permeate, there was no visible precipitation, and thus there could have been no protein in the permeate. Hopefully, a repetition of this rejection study and more careful analysis will show this indication to be true.